

We are IntechOpen, the world's leading publisher of Open Access books Built by scientists, for scientists

6,900

Open access books available

186,000

International authors and editors

200M

Downloads

Our authors are among the

154

Countries delivered to

TOP 1%

most cited scientists

12.2%

Contributors from top 500 universities



WEB OF SCIENCE™

Selection of our books indexed in the Book Citation Index
in Web of Science™ Core Collection (BKCI)

Interested in publishing with us?
Contact book.department@intechopen.com

Numbers displayed above are based on latest data collected.
For more information visit www.intechopen.com



Electric Motor Performance Improvement Using Auxiliary Windings and Capacitance Injection

Nicolae D.V
Tshwane University of Technology
South Africa

1. Introduction

Generally, some electric machines such as induction machines and synchronous reluctance motors require reactive power for operation. While the reactive power required by a synchronous machine can be taken from the power source or supplied by the machine itself by adjustment of the field current, the power factor of an induction machine is always lagging and set by external quantities (i.e., the load and terminal voltage). Poor power factor adversely affects the distribution system and a cost penalty is frequently levied for excessive VAR consumption.

Power factor is typically improved by installation of capacitor banks parallel to the motor. If the capacitor bank is fixed (i.e. that it can compensate power factor only for a fixed load), when the load is variable, then the compensation is lost. Some authors (El-Sharkawi *et al.*, 1984, Fuchs and Hanna, 2002) introduced the capacitors using thyristor/triac controllers; by adjusting the firing angle, the capacitance introduced in parallel with the motor becomes variable and thus compensating the power factor for any load. Other works (Suciu *et al.*, 2000.) consider the induction motor as an RL load and power factor is improved by inserting a variable capacitor (through a bridge converter) which is adjusted for unity according with the load. For the above methods, the capacitive injection is directly into the supply. Another method conceived for slip ring induction motor was to inject capacitive reactive power direct into the rotor circuit (Reinert and Parsley, 1995; Suciu, *et al.* 2002).

The injection of reactive power can be done through auxiliary windings magnetically coupled with the main windings (E. Muljadi *et al.* 1989; Tamrakan and Malik, 1999; Medarametla *et al.* 1992; Umans, and H. L. Hess, 1983; Jimoh and Nicolae, 2006, 2007). This compensating method has also been applied with good results not only for induction motors but also for a synchronous reluctance motor (Ogunjuyigbe *et al.* 2010).

2. Method description

2.1 Physical solution

The method described in this chapter makes use of two three-phase stator windings. One set, the main winding (star or delta), is connected directly to the source. The other set of windings - auxiliary, is only magnetically coupled to the main winding. All windings have the same shape and pitch, but may have different turn numbers and wire sizes; usually smaller in order to be accommodated in the slots together with the stator. The windings are

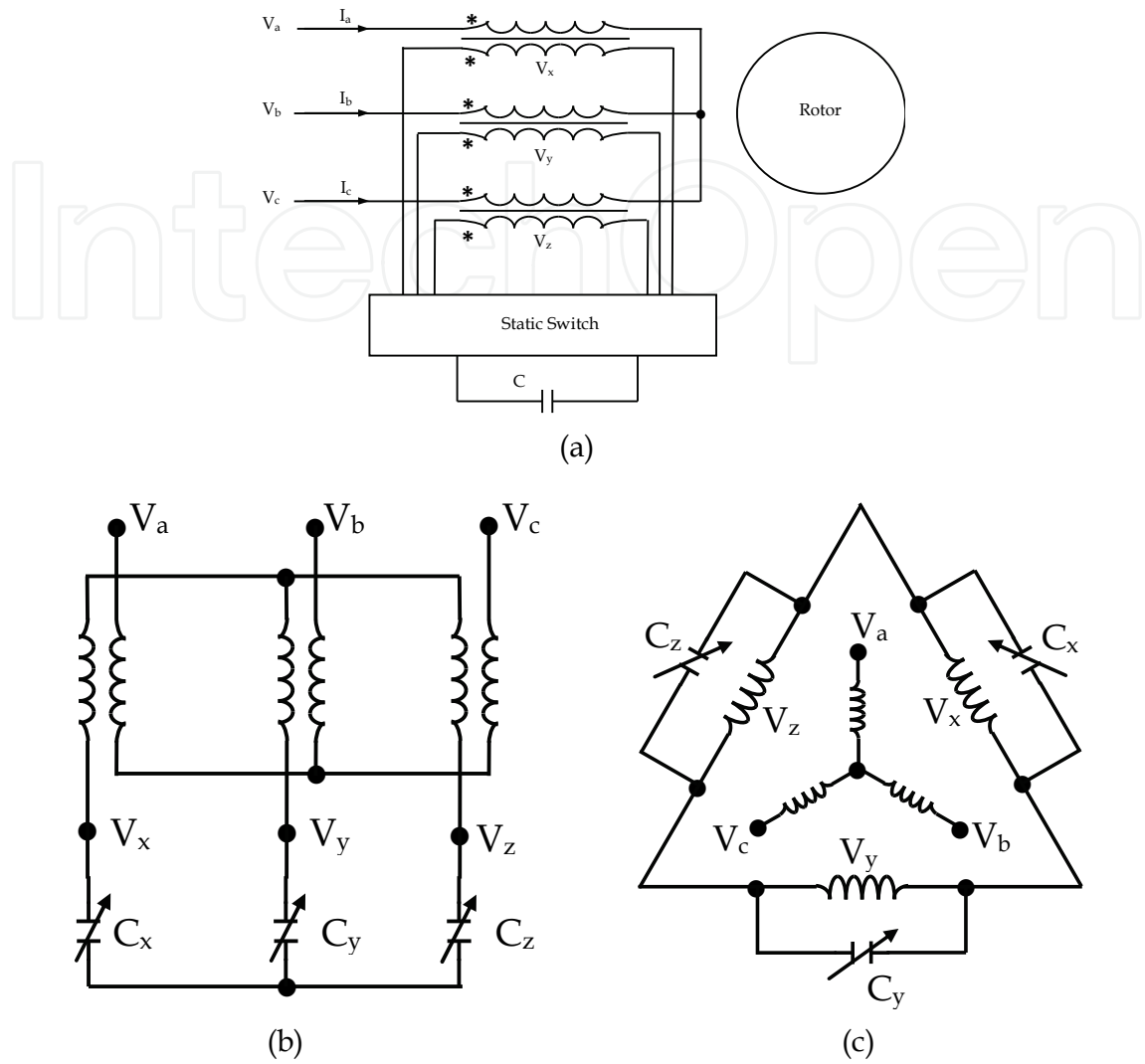


Fig. 2. Auxiliary windings: a) generic connection; b) star connection; c) delta connection

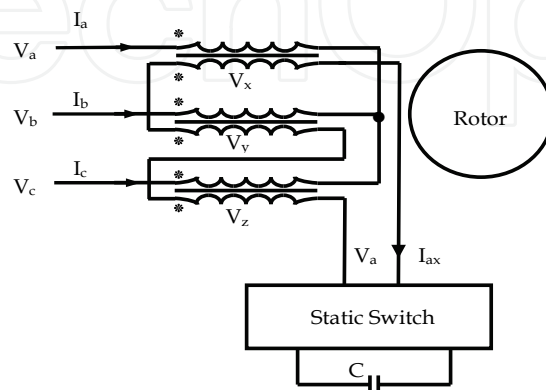


Fig. 3. Auxiliary windings: "single-phase connection"

2.3.1 Thyristor-based variable capacitor

Figure 4 shows the use of thyristor to accomplish a variable capacitor. The inductor L_r is introduced to reduce - limit the surge current; it is relatively small and does not affect the overall capacitive behaviour.

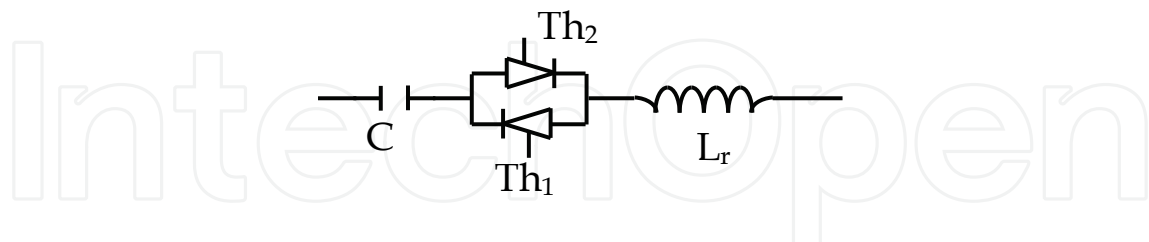


Fig. 4. Variable capacitor using bidirectional thyristor

The equivalent capacitance depends on the delay angle. Due to the phase angle control, the device introduces harmonic currents.

2.3.2 IGBT-based variable capacitor

The above drawback can be address using IGBTs in bidirectional configuration (Figure 5) and a switching frequency higher then operational frequency (50 Hz).

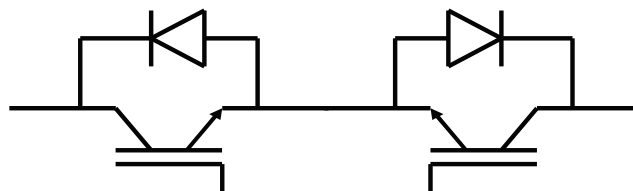


Fig. 5. IGBT in bidirectional topology

Figure 6 shows a configuration to achieve a variable capacitor using two bidirectional static switches. The main capacitor C_1 is introduced in the auxiliary winding circuit, via a bidirectional switch Sw_1 , for a period of time depending on the duty cycle (δ) of the switching frequency; in this time the bidirectional switch Sw_2 is OFF. When Sw_1 is OFF, the capacitor is discharged. The reactor L_r limits the capacitive surge current without affecting the capacitive behaviour.

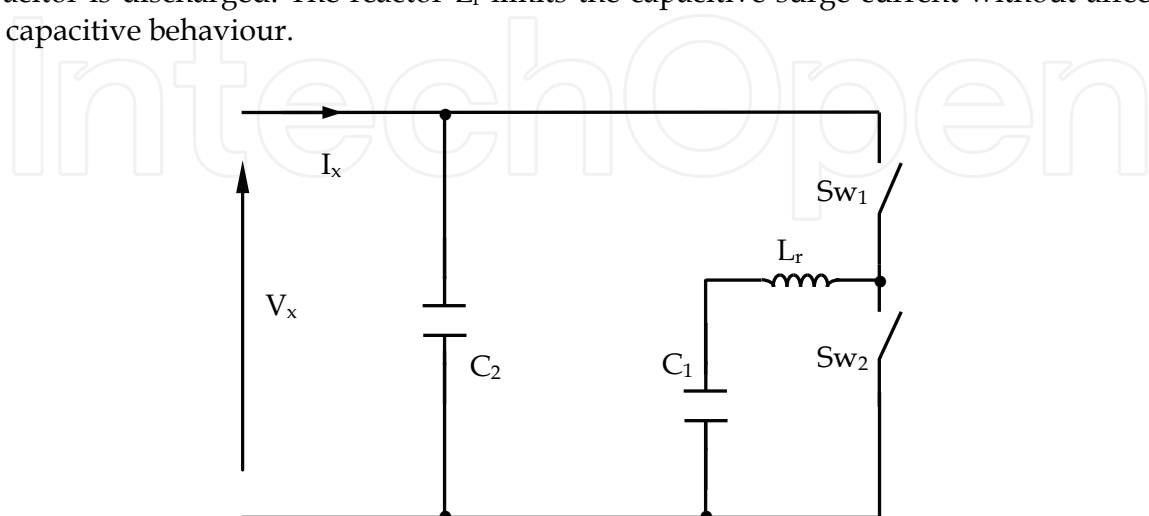


Fig. 6. Variable capacitor using two IGBTs in bidirectional topology

The capacitor C_2 , much smaller than C_1 is connected to mitigate the voltage spikes during switching off the main capacitor. Thus, the equivalent capacitor can be written as:

$$C_{eq} = \delta \times C_1 + C_2 \quad (1)$$

2.3.3 Variable capacitor H-topology

Figure 7 shows a **single-phase H topology** to achieve a variable capacitor. This configuration using H-bridge bidirectional topology obtains a higher equivalent capacitance for the same fixed one as reference. In this configuration, the reactor L_r has the same purpose of limiting the surge capacitive current, while C_2 also of small value mitigates the voltage spikes. The equivalent capacitance could be express as:

$$C_{eq} = C_2 + \frac{C_1}{(2\delta - 1)^2} \quad (2)$$

It can be notice that the equivalent capacitance could increase significant when the duty cycle approaches 50 %. In practice, the switches are not ideal and there is no "infinite increase" of the equivalent capacitance.

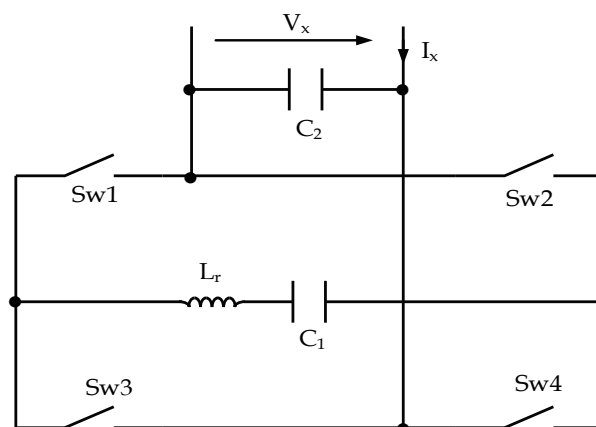


Fig. 7. Variable capacitor using H-bridge bidirectional topology

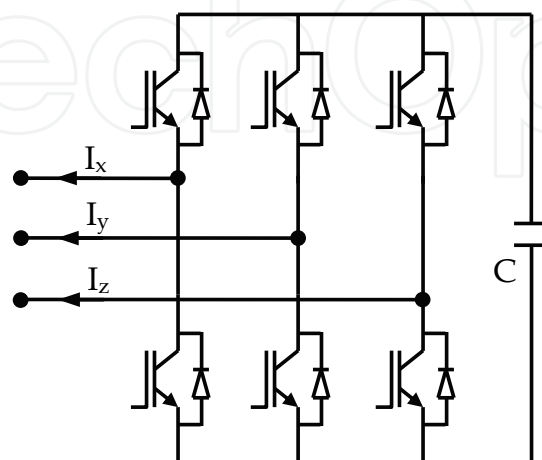


Fig. 8. Variable capacitor using three-phase H-bridge topology

Another solution to achieve a variable capacitance, or rather to generate a capacitive current was proposed using a **three-phase H topology** as PWM inverter (E. Muljadi, *et al* 1989; Tamrakan and Malik, 1999) as presented in Figure 8. The converter injects capacitive reactive power into auxiliary windings and thus improving the power factor of the motor.

3. Mathematical model

The machine is treated as having two three-phase windings and the voltages equations system can be written as:

$$[V_{abcs}] = [R_1][I_{abc}] + \frac{d}{dt}[\lambda_{abc}] \quad (3)$$

$$0 = [R_2][I_{xyz}] + \frac{d}{dt}[\lambda_{xyz}] + V_{c_{xyz}} \quad (2)$$

$$0 = [R_r][I_{abcr}] + \frac{d}{dt}[\lambda_{abcr}] \quad (5)$$

where

$$V_{abc} = [V_a \quad V_b \quad V_c]^T \quad (6)$$

$$I_{abcs} = [I_a \quad I_b \quad I_c]^T; \quad \lambda_{abc} = [\lambda_a \quad \lambda_b \quad \lambda_c]^T \quad (7)$$

$$[R_1] = \begin{bmatrix} r_a & 0 & 0 \\ 0 & r_b & 0 \\ 0 & 0 & r_c \end{bmatrix} \quad [R_2] = \begin{bmatrix} r_x & 0 & 0 \\ 0 & r_y & 0 \\ 0 & 0 & r_z \end{bmatrix} \quad (8)$$

Note that indices "1" refer to the main winding and "2" to the auxiliary winding.

$$\begin{bmatrix} \lambda_{abcs} \\ \lambda_{xyz} \\ \lambda_{abcr} \end{bmatrix} = \begin{bmatrix} L_{abc} & L_{abcsxyz} & L_{abcsr} \\ L_{xyzabcs} & L_{xyz} & L_{xyzabcr} \\ L_{abcrs} & L_{abcrxyz} & L_{abcr} \end{bmatrix} \begin{bmatrix} I_{abcs} \\ I_{xyz} \\ I_{abcr} \end{bmatrix} \quad (9)$$

The inductances in eq. (9) are time dependent, and this make the equation difficult and time consuming to solve. In order to obtain constant parameters, the voltage equations (3-5) are then transformed to the rotor reference frame. To achieve this, the equations are multiplied with an appropriate transformation matrix $K(\theta)$ to obtain:

$$[K(\theta)][V_{abcs}] = [R_1][K(\theta)][I_{abcs}] + \frac{d}{dt}[K(\theta)][\lambda_{abcs}] \quad (10)$$

$$0 = [R_2][K(\theta)][I_{xyzs}] + \frac{d}{dt}[K(\theta)][\lambda_{xyzs}] + [K\theta][V_{cxyzs}] \quad (11)$$

$$0 = [R_r][K(\theta_r)][I_{abcr}] + \frac{d}{dt}[K(\theta_r)][\lambda_{abcr}] \tag{12}$$

When these equations are expanded, after substantial matrix manipulations, it resolves to:

$$[V_{qdo1}] = [R_{s1}][I_{qdo1}] + \frac{d}{dt}[\lambda_{qd01}] + \varpi[\lambda_{qd01}] \tag{13}$$

$$0 = [R_2][I_{qdo2}] + \frac{d}{dt}[\lambda_{qd02}] + \varpi[\lambda_{qd02}] + [V_{C_{qd02}}] \tag{14}$$

$$0 = [R_r][I_{qdor}] + \frac{d}{dt}[\lambda_{qd0r}] + \varpi_r[\lambda_{qd01}] \tag{15}$$

where

$$\varpi = \omega \begin{bmatrix} 0 & 1 & 0 \\ -1 & 0 & 0 \\ 0 & 0 & 0 \end{bmatrix}; \varpi_r = (\omega - \omega_r) \begin{bmatrix} 0 & 1 & 0 \\ -1 & 0 & 0 \\ 0 & 0 & 0 \end{bmatrix} \tag{16}$$

and

$$[V_{C_{qd02}}] = \frac{1}{C} \int [I_{qd02}] dt + \varpi [V_{C_{qd02}}] \tag{17}$$

Neglecting the '0' sequence since we initially are assuming a balanced system, the expression for the stator and rotor flux linkages, resolves into the matrix:

$$\begin{bmatrix} \lambda_{q1} \\ \lambda_{d1} \\ \lambda_{q2} \\ \lambda_{d2} \\ \lambda_{qr} \\ \lambda_{dr} \end{bmatrix} = \begin{bmatrix} L_{ls1} + L_m & 0 & L_{lm} + L_m & 0 & L_m & 0 \\ 0 & L_{ls1} + L_m & 0 & L_{lm} + L_m & 0 & L_m \\ L_{lm} + L_m & 0 & L_{ls2} + L_m & 0 & L_m & 0 \\ 0 & L_{lm} + L_m & 0 & L_{ls2} + L_m & 0 & L_m \\ L_m & 0 & L_m & 0 & L_{lsr} + L_m & 0 \\ 0 & L_m & 0 & L_m & 0 & L_{lsr} + L_m \end{bmatrix} \begin{bmatrix} I_{q1} \\ I_{d1} \\ I_{q2} \\ I_{d2} \\ I_{qr} \\ I_{dr} \end{bmatrix} \tag{18}$$

4. Equivalent model

4.1 Symmetrical loaded auxiliary windings

When each phase of the auxiliary windings is loaded with equal capacitors (C), eventually star connected, the entire circuit is having a symmetrical behaviour and the equivalent circuit is very simple as shown in Figure 9.

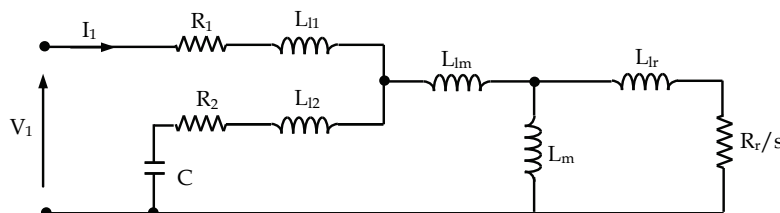


Fig. 9. Equivalent circuit for symmetrical loading auxiliary winding

This equivalent circuit has two branches, each having separate resistance (R_1 - main and R_2 - auxiliary) and leakage reactance (L_{l1} - main and L_{l2} - auxiliary) together with a common mutual leakage inductance L_{lm} , which occurs due to the fact that the two set of windings occupy the same slots and therefore mutually coupled by their leakage flux. The mutual inductance that occurs between main winding and rotor is represented by L_m .

Other parameters of the equivalent circuit are: main winding resistance R_1 , auxiliary winding resistance R_2 , main winding leakage reactance L_1 , auxiliary winding leakage inductance L_2 ; mutual leakage inductance L_{lm} , rotor leakage inductance L_{lr} ; and the rotor resistance R_r and "s" is the slip.

In this analysis there is no need to refer the auxiliary winding quantities to the main winding, because the two sets of windings are wound for the same number of turns with a transformation ratio of one.

The above equivalent circuit helps us to determine the input impedance seen from the supply and the condition for unity power factor.

$$Z_{in} = R_1 + jX_{l1} + \frac{(R_2 R_3 - X_2 X_3) + j(X_2 R_3 + X_3 R_2)}{(R_2 + R_3) + j(X_2 + X_3)} \quad (19)$$

Where: R_1 and jX_{l1} are the components of the main winding (per-phase impedance), X_2 is the equivalent reactance of the auxiliary winding including the compensating capacitor, R_2 is the resistance (per-phase) of the auxiliary winding, R_3 and X_3 are the equivalent resistance and reactance of the paralleling the rotor branch with magnetizing branch:

$$X_2 = \frac{1}{\omega C} - X_{l2} \quad (20)$$

$$X_3 = \text{Im} \left\{ jX_{lm} + \left[\frac{(R_r/s) + jX_{lr}}{jX_m} \right] \right\} \quad (21)$$

$$R_3 = \text{Re} \left\{ \left[\frac{(R_r/s) + jX_{lr}}{jX_m} \right] \right\} \quad (22)$$

The condition for unity power factor is:

$$\text{Im} \{ Z_{in} \} = 0 \quad (23)$$

Which, after some mathematical manipulation can be written as:

$$\alpha X_2^2 + \beta X_2 + \gamma = 0 \quad (24)$$

With:

$$\alpha = X_3 + X_{l1} \quad (25)$$

$$\beta = -R_2 R_3 + (R_1 + R_2) R_3 + 2X_3 X_{l1} \quad (26)$$

$$\gamma = -X_3 \left[R_2 R_3 - (R_2 + R_3) R_1 \right] + X_{l1} \left[(R_2 + R_3)^2 + X_3^2 \right] \quad (27)$$

The equation (24) together with relations (25) to (27) produces two solutions, which means for a given slip (s) there are two values for the capacitor satisfying the condition for unity power factor. The practical/recommended value is the high X_2 or small C connected to the auxiliary winding in order to have a small current through it.

4.2 Asymmetrical loaded auxiliary windings.

If the auxiliary windings are connected as “single-phase configuration”, then the system has an asymmetrical behaviour. This connection is obtained by connecting in series the three auxiliary windings and thus we can write: $I_x = I_y = I_z = I_X$. Using this condition of current in the expansion that results to equations (3) - (18) it can be written: $I_{d2} = I_{q2} = 0$, thus the resulting expression from this can be represented in a d-q-0 equivalent circuit of Figure 10 shown below.

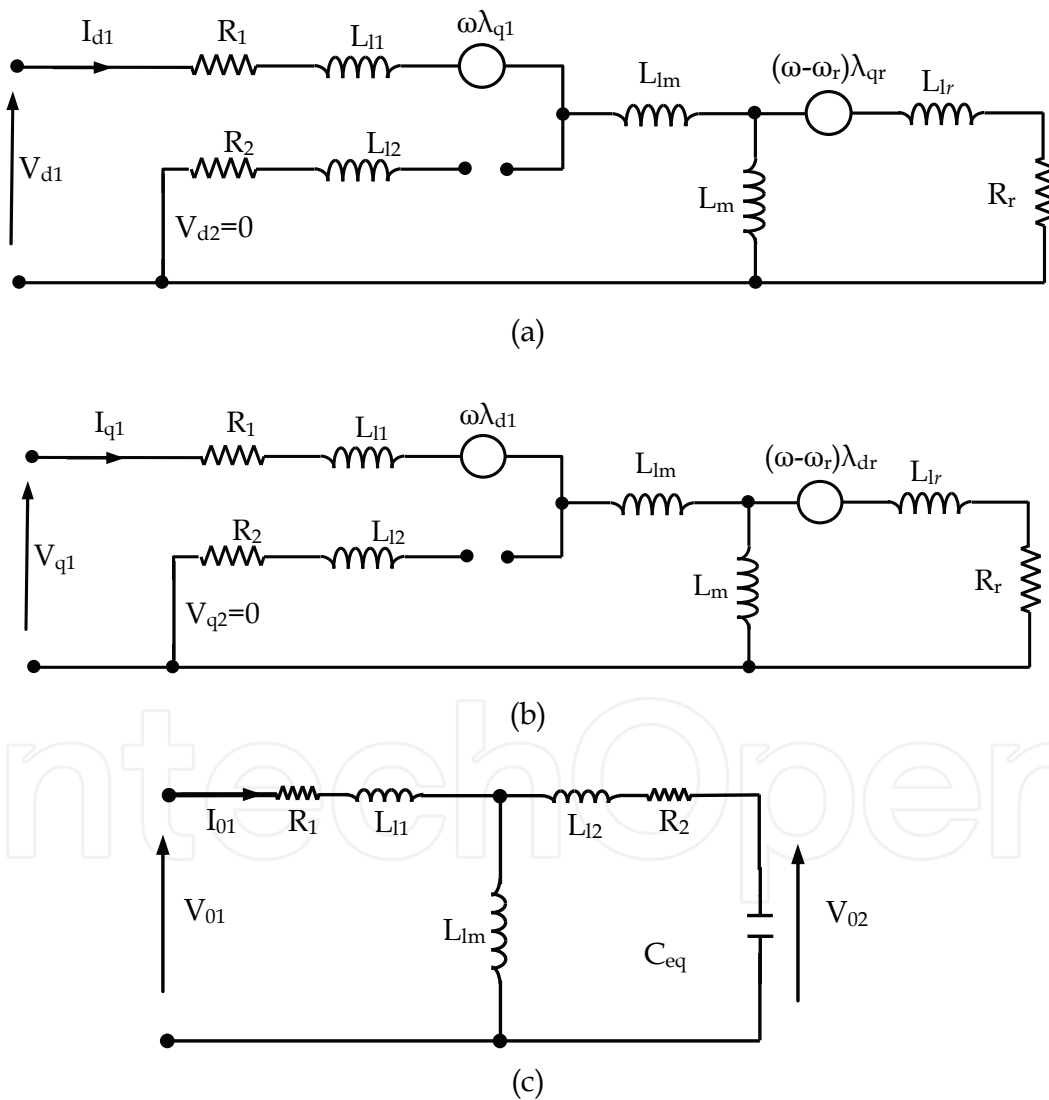


Fig. 10. The “d-q-0” equivalent circuit: a) “d” - equivalent circuit; b) “q” - equivalent circuit; c) “0” - equivalent circuit

The particularity of connecting the auxiliary windings in a single phase winding creates an asymmetrical situation which brings about the relevance of the zero sequence.

The power factor of the machine could be defined by the argument of Z_a , which is V_a/I_a . And this is expressed as:

$$Z_a = \frac{V_a}{I_a} = \frac{V_{q1} + V_{01}}{I_{q1} + I_{01}} \quad (28)$$

$$V_{01}(C) = (-j\omega C + Z_{02}) \times I_{02} \times \frac{(Z_{01} + Z_{lm})}{Z_{lm}} \quad (29)$$

As can be observed from the equations (28) and (29), the power factor of the machine depends on C and thus it can be brought to unity by means of adjusting the equivalent capacitance.

It should be also noticed that the asymmetrical behaviour of the auxiliary windings connected as "single-phase configuration" has got a significant draw-back namely creating torque ripple. This disadvantage should not be overseen by the simplicity of the physical solution. Given this, further in this, we will consider only the symmetrical loading of the auxiliary winding.

5. Concept validation

For the validation of this concept of improving performances of the induction motor injecting capacitive reactive power via auxiliary windings, a standard 4 kW, 380V, 50Hz, 4 pole, 36 slots with frame size DZ113A induction motor have been used. The stator was rewound with two full-pitches, single layer windings (see Figure 1). The main windings - delta connected have same number of turns like in the original motor but the size of the wire has been reduced to accommodate the auxiliary windings. The auxiliary windings were connected in delta in order to reduce current through them. For this study, the auxiliary windings have the same number of turns as main windings. The rotor is unchanged. Table 1 shows the parameters of the modified motor under test obtained using the IEEE test procedure. The mutual leakage inductance X_{lm} is very small compared to the other reactance's (E. Muljadi et al, 1989).

Description of data	Values
Main Winding Rated Voltage	380 V
Auxiliary Winding Rated Voltage	380V
Number of poles	4
Magnetizing Reactance (X_m)	37.86 Ω
Main winding phase resistance (R_1)	4.33 Ω
Auxiliary winding phase resistance (R_2)	18.1 Ω
Main winding leakage reactance (X_{l1})	6.97 Ω
Auxiliary winding leakage reactance (X_{l2})	6.97 Ω
Rotor resistance (R_r)	1.35 Ω
Rotor leakage reactance (X_{lr})	1.97 Ω
Full load main winding current	8.6 A

Table 1. Specific parameters of the induction motor under test

Firstly, the motor was tested without compensation; the results are presented in Table 2.

I_L (A)	T_L (Nm)	P(W)	S(VA)	PF	Slip	RPM
5.43	1.83	678.6	3568.7	0.17	0.0026	1496
5.56	4.73	1734	3655.1	0.43	0.0060	1491
6.02	5.49	1992	3957.5	0.49	0.0086	1487
6.88	7.53	2709	4522.9	0.61	0.0153	1477
7.74	9.89	3540	5088.2	0.70	0.0213	1468
8.61	12.1	4179	5653.6	0.74	0.056	1416

Table 2. Experimental data for the motor under test

5.1 Simulation results

Based on Matlab platform, a simulation model has been built (Figure 11). The parameters from Table 1 have been used for Matlab model after delta-star transformation.

The rotor resistor was simulated using a variable resistor depending on slip. The model was run firstly to show the capability of adjusting the power factor via the static switch.

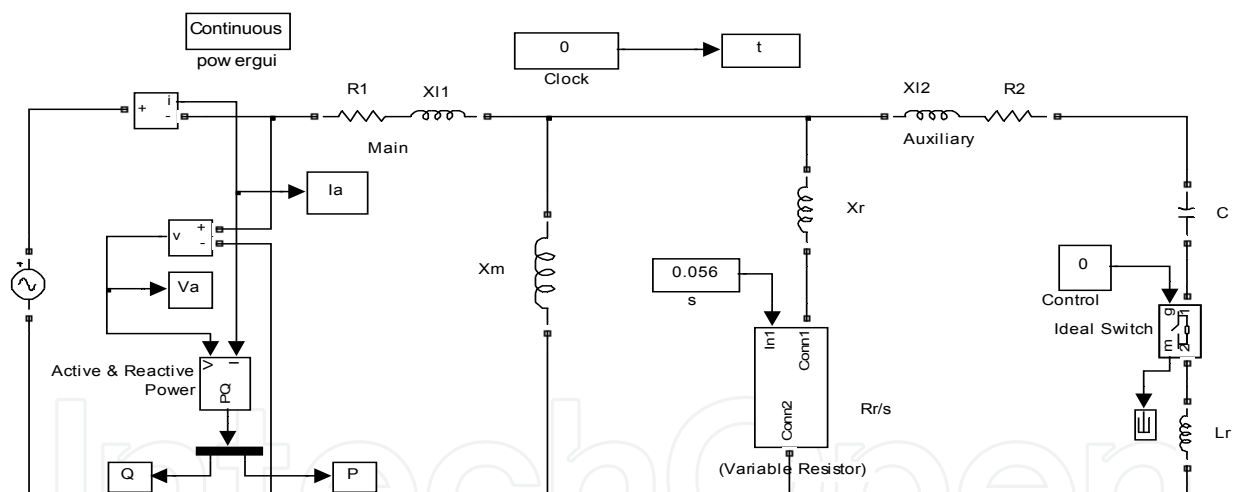


Fig. 11. Basic simulation model

5.1.1 Thyristor-based variable capacitor

One of the first solutions to introduce a variable capacitor was to use an “ac-ideal” switch based on two thyristors anti-parallel connected. The test was done using a 100 μ F and a delay angle of 45° for a slip of 0.0026 (no load). This results in a reduction of reactive power drawn by the motor from 1193 VAR to 46 VAR. The main drawback of this switching solution is the strong distorting currents introduced as could be seen in Figure 12.

As could be noticed, both currents main and auxiliary are very much distorted. Obviously, the power factor compensation is accompanied with degrading of all other performances of the motor.

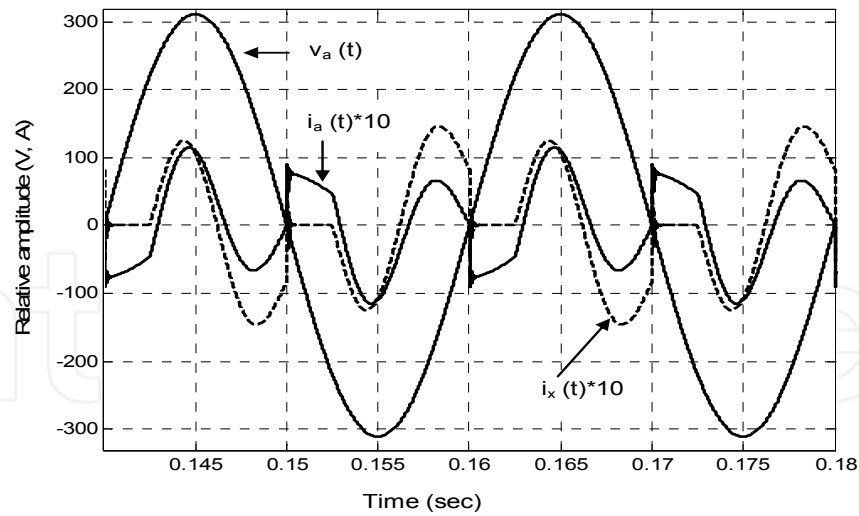


Fig. 12. Electric parameters (v_a , i_a and i_x) for compensated model using thyristor-based variable capacitor

5.1.2 IGBT-based variable capacitor

The other solution tested to obtaining variable capacitor was that of Figure 6. The values for the two capacitors were chosen as: $C_1 = 100 \mu\text{F}$ and $C_2 = 1 \mu\text{F}$. The validation simulation was done for a slip of $s = 0.0026$; the switching frequency was 1 kHz and then the duty cycle manually adjusted. Figure 13 shows the main and auxiliary currents toward supply voltage for a duty cycle of 40 % (Fig.13. a) and 80% (Fig.13. a).

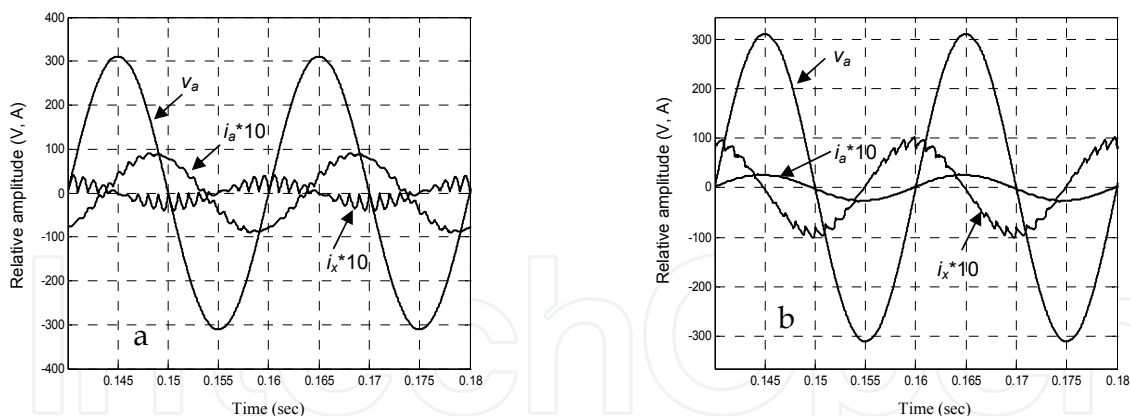


Fig. 13. Main and auxiliary currents for $s = 0.0026$, 1 kHz and: a) $\delta = 40 \%$; b) $\delta = 80 \%$.

As can be noticed a duty cycle of 40 % does adjust the shift between the main current and voltage marginally increasing the power factor from 0.15 to 0.32 lagging. When the duty cycle was increased to 80%, then the main current arrived in phase with the voltage. It can also be noticed a relative high ripple especially for low duty cycle.

Figure 14 shows the same simulation conditions, but now the switching frequency was raised to 4 kHz. As can be noticed the ripple has been reduced significant.

The other methods of producing variable capacitive reactive power, meaning the H-bridge topologies require a more complex control system and are not addressed in this study.

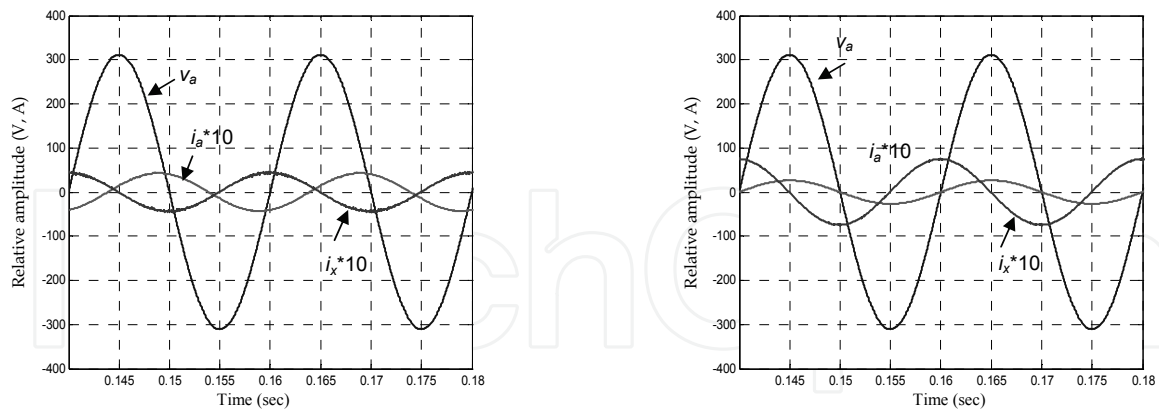


Fig. 14. Main and auxiliary currents for $s = 0.0026$, 4 kHz and: a) $\delta = 40\%$; b) $\delta = 80\%$.

5.1.3 Capacitance versus slip for unity power factor

Now, the model was run for each value of the slip (speed) given in Table 2. The result of these simulations is the capacitance producing unity power factor (see Table 3).

s (n)	C_Y (μF)	I_a (A)	P_a (W)	Q_a (VAr)	S_a (VA)	PF
0.0026 (1496)	0	5.49	184	1193	1207	0.152
	81	1.65	362	9	363	0.999
0.006 (1491)	0	5.65	366	1187	1242	0.295
	81	2.57	565	11	565	0.999
0.0086 (1487)	0	5.86	505	1186	1289	0.392
	81.6	3.27	718	15	719	0.999
0.0153 (1477)	0	6.71	855	1200	1473	0.58
	87	5.21	1143	1	1143	0.999
0.0213 (1468)	0	7.68	1160	1229	1689	0.686
	90	6.82	1499	17	1499	0.999
0.056 (1491)	0	8.31	1330	1252	1826	0.728
	90.6	7.66	1684	27	1686	0.999

Table 3. Simulation results: capacitance versus slip for unity power factor

It is interesting to observe that the capacitance producing unity power factor does not vary so much as presented in other studies (E. Muljadi *et al.* 1989; Tamrakan and Malik, 1999) concerning similar method of injecting capacitive reactive power.

Moreover, it could be found a fix value of $75\ \mu\text{F}$ which maintain a high power factor irrespective of the load/slip. Table 4 shows the simulation results for the fixed capacitor and variable load/slip.

Figure 15 shows the variation of the power factor versus slip and Figure 16 shows the variation of the supply current versus slip for compensated with a fix $75\ \mu\text{F}$ capacitor per phase and uncompensated machine.

s	C_Y (μF)	I_a (A)	P_a (W)	Q_a (VAr)	S_a (VA)	PF
0.0026	75	1.57	330	101	345	0.956
0.006	75	2.47	531	111	542	0.978
0.0086	75	3.16	683	123	694	0.984
0.0153	75	4.91	1066	170	1079	0.987
0.0213	75	6.44	1396	230	1415	0.987
0.056	75	7.29	1580	272	1603	0.986

Table 3. Simulation results: capacitance versus slip for unity power factor

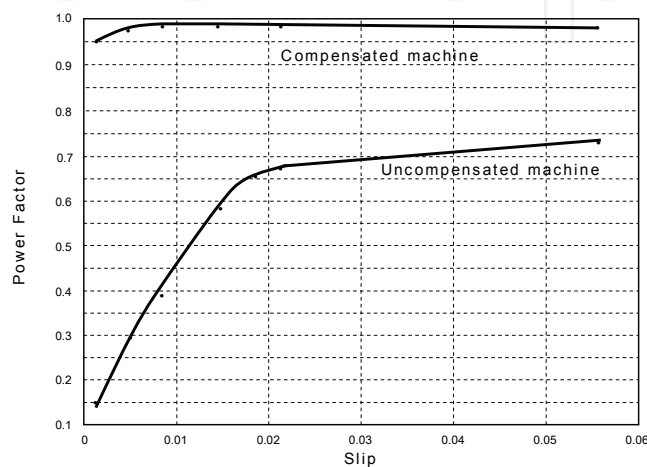


Fig. 15. Power Factor versus slip

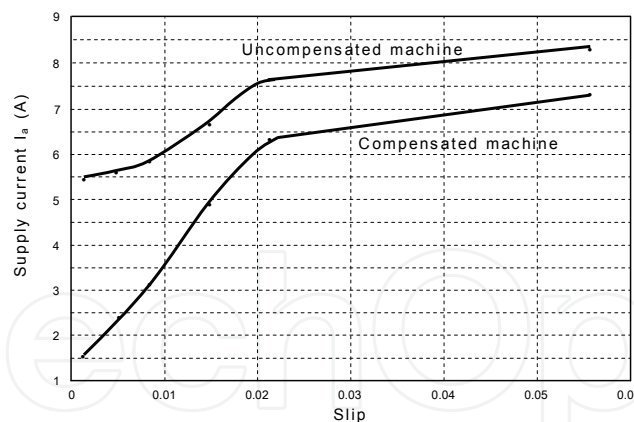


Fig. 16. Supply current versus slip

5.2 Experimental validation

After rewinding the machine under test with both sets of windings delta connected, three identical capacitors were connected to the auxiliary. Then the “compensated” motor was loaded gradually to get the same speeds as for the “uncompensated” motor.

The testing started with a capacitance of $25 \mu\text{F}$ as found during the simulation: $C_\Delta = C_Y / 3$. This did not produce the results found via the simulation. Then a value of $28 \mu\text{F}$ was found to give a relative even power factor of approximate 0.95 in the entire loading range (see Table 4).

Figure 17 shows the phase voltage (v_{an}) and current (i_a) for the uncompensated (Fig. 17.a) and compensated (Fig. 17.b) with slip of 0.0026. It can be observed, the power factor increased from 0.17 to 0.937 which represent 450% improvement for no load. For full load the improvement in power factor is 29%.

I_L (A)	T_L (Nm)	P(W)	S(VA)	PF	Slip	RPM
1.71	2.81	1058	1129	0.937	0.0026	1496
2.71	4.73	1694	1789	0.947	0.0060	1491
3.49	5.83	2191	2304	0.951	0.0086	1487
5.46	7.63	2709	3604	0.955	0.0153	1477
6.92	9.29	3442	4567	0.952	0.0213	1468
7.85	13.8	4937	5181	0.953	0.056	1416

Table 2. Experimental data for the motor under test

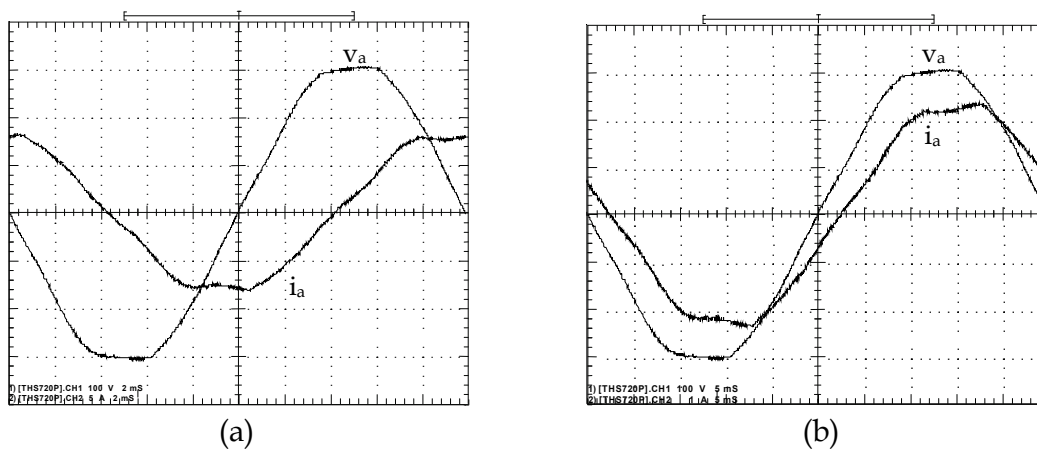


Fig. 17. Voltage and current for: a) uncompensated motor; b) compensated motor

6. Comments

This study proved that direct injecting capacitance reactance through auxiliary winding does improve the power factor of the induction motor; it also increases the ratio torque over current. What is also very interesting is this method achieves a “flat” variation of power factor with respect of load variation. This is a very important improvement given the fact that majority of induction motors do not work at constant full load where the classic design produces maximum performances.

However, this method introduces extra copper losses reducing the overall efficiency and increasing the operation temperature.

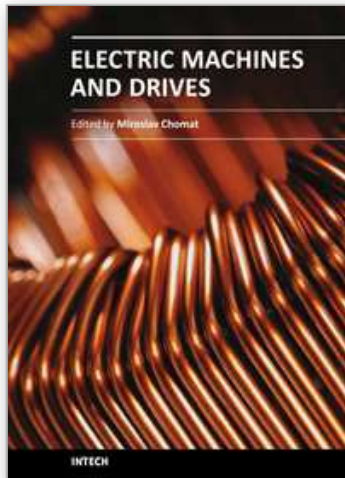
This study did not intended to elucidate the full effect of the method upon the torque especially the existence of the influence produced by the current flowing through auxiliary windings. The only aspect clearly noticed was the torque ripple introduced by the “single-phase” auxiliary winding connection.

Further more, the same method was applied to a synchronous reluctance motor (Ogunjuyigbe *et al*, 2010). The same type of stator winded similarly as above was used with a salient milled rotor obtained from the corresponding squirrel cage induction motor. The experimental results show an improvement of the power factor from 0.41-0.69 to 0.93-0.97 for the entire loading range.

The economic benefits are related with the savings on demand especially for places where a large number of three-phase induction motors are used under variable loading.

7. References

- M. A El-Sharkawi, S. S Venkata, T. J Williams, and N. G Butler, "An adaptive Power Factor Controller for Three-Phase Induction Generators", Paper 84 SM 672-2 presented at the *IEEE/PES Summer Meeting*, Seattle, Washington, July 15-20, 1984.
- Fuchs, E.F. Hanna, W.J.; "Measured efficiency improvements of induction motors with thyristor/triac controllers", , *IEEE Transaction on Energy Conversion*, Volume 17, Issue 4, Dec. 2002 pp. 437 - 444
- Suciu, C.; Dafinca, L.; Kansara, M.; Margineanu, I.; "Switched capacitor fuzzy control for power factor correction in inductive circuits", *IEEE 31st Annual Power Electronics Specialists Conference*, 2000. Vol. 2, pp. 773 - 777
- C. Suciu, M. Kansara, P. Holmes and W. Szabo, "Performance Enhancement of an Induction Motor by Secondary Impedance Control, *IEEE Trans. On Energy Conversion*, Vol. 17, No. 2, June 2002
- J. Reinert, M.J. Parsley, "Controlling the speed of 8×1 induction motor by resonating the rotor & wit," in *IEEE Transactions on Industry Applications*, Vol. 31, No. 4, July/August 1995, pp. 887-891.
- E. Muljadi, T.A. Lipo, D.W. Novotny, "Power Factor Enhancement of Induction Machines by Means of Solid State Excitation," *IEEE Trans. on Power Electronics*, Vol. 4, No. 4, pp. 409418, Oct. 1989.
- I. M Tamrakan and O.P Malik, "Power Factor Correction of Induction motors Using PWM Inverter Fed Auxiliary Stator Winding", *IEEE Transaction on Energy Conversion*, Vol. 14, No.3, Sept, 1999, pp. 426-432
- J. B. Medarametla, M. D. Cos, and Baghzouz, "Calculations and measurement of unity plus three-phase induction motor," *IEEE Transactions on Energy Conversion*, vol. 7, no. 4, pp. 732-738, 1992.
- S. D. Umans, and H. L. Hess, "Modelling and analysis of a the Wanlass three-phase induction motor configuration," *IEEE Transaction on Power Apparatus and Systems*, vol. 102, no. 9, pp. 2912-2916, 1983.
- R. Spée and A. Wanllace, "Comparative Evaluation Of Power-Factor Improvement Techniques For Squirrel cage Induction Motors", *Industry Applications Society Annual Meeting*, 1990.
- A.A. Jimoh and D.V. Nicolae, "Performance Analysis of a Three-Phase Induction Motor with Capacitance Injection", *OPTIM'06*, 10th International Conference on Optimization of Electrical and Electronic Equipments, Brasov, Romania, May 17-20, 2006
- D.V. Nicolae and A.A. Jimoh, "Three-Phase Induction Motor with Power Electronic Controlled Single-Phase Auxiliary Stator Winding", *PESC'07*, The 38th IEEE Power Electronics Specialists Conference, Orlando, USA, June 17-21, 2007
- A.S.O. Ogunjuyigbe, A.A. Jimoh, D.V. Nicolae and E.S. Obe, "Analysis of Synchronous Reluctance Machine with Magnetically Coupled Three Phase Windings and Reactive Power compensation", *IET Electric Power Applications*, 2010, Vol. 4, Iss. 4, pp 291-303



Electric Machines and Drives

Edited by Dr. Miroslav Chomat

ISBN 978-953-307-548-8

Hard cover, 262 pages

Publisher InTech

Published online 28, February, 2011

Published in print edition February, 2011

The subject of this book is an important and diverse field of electric machines and drives. The twelve chapters of the book written by renowned authors, both academics and practitioners, cover a large part of the field of electric machines and drives. Various types of electric machines, including three-phase and single-phase induction machines or doubly fed machines, are addressed. Most of the chapters focus on modern control methods of induction-machine drives, such as vector and direct torque control. Among others, the book addresses sensorless control techniques, modulation strategies, parameter identification, artificial intelligence, operation under harsh or failure conditions, and modelling of electric or magnetic quantities in electric machines. Several chapters give an insight into the problem of minimizing losses in electric machines and increasing the overall energy efficiency of electric drives.

How to reference

In order to correctly reference this scholarly work, feel free to copy and paste the following:

Nicolae D.V (2011). Electric Motor Performance Improvement Using Auxiliary Windings and Capacitance Injection, Electric Machines and Drives, Dr. Miroslav Chomat (Ed.), ISBN: 978-953-307-548-8, InTech, Available from: <http://www.intechopen.com/books/electric-machines-and-drives/electric-motor-performance-improvement-using-auxiliary-windings-and-capacitance-injection>

INTECH
open science | open minds

InTech Europe

University Campus STeP Ri
Slavka Krautzeka 83/A
51000 Rijeka, Croatia
Phone: +385 (51) 770 447
Fax: +385 (51) 686 166
www.intechopen.com

InTech China

Unit 405, Office Block, Hotel Equatorial Shanghai
No.65, Yan An Road (West), Shanghai, 200040, China
中国上海市延安西路65号上海国际贵都大饭店办公楼405单元
Phone: +86-21-62489820
Fax: +86-21-62489821

© 2011 The Author(s). Licensee IntechOpen. This chapter is distributed under the terms of the [Creative Commons Attribution-NonCommercial-ShareAlike-3.0 License](#), which permits use, distribution and reproduction for non-commercial purposes, provided the original is properly cited and derivative works building on this content are distributed under the same license.

IntechOpen

IntechOpen